

We are IntechOpen, the world's leading publisher of Open Access books Built by scientists, for scientists

6,900

Open access books available

186,000

International authors and editors

200M

Downloads

Our authors are among the

154

Countries delivered to

TOP 1%

most cited scientists

12.2%

Contributors from top 500 universities



WEB OF SCIENCE™

Selection of our books indexed in the Book Citation Index
in Web of Science™ Core Collection (BKCI)

Interested in publishing with us?
Contact book.department@intechopen.com

Numbers displayed above are based on latest data collected.
For more information visit www.intechopen.com



Fracture Toughening Mechanisms in Epoxy Adhesives

Aldobenedetto Zotti, Simona Zuppolini,
Mauro Zarrelli and Anna Borriello

Additional information is available at the end of the chapter

<http://dx.doi.org/10.5772/65250>

Abstract

Fracture toughness is generally considered as the main properties of a polymer or a polymer adhesive system for measuring the material resistance to the extension of cracks. Epoxy adhesives are generally brittle in nature; however, the addition of a second dispersed phase could induce a remarkable increase of damage tolerance performance by an enhancement of the material fracture toughness. The fracture behavior of a filled epoxy resin is strongly affected by the dimensions, the shape, and the chemical nature of the considered filler. The chapter describes the different toughening mechanisms for polymer adhesives with special attention toward innovative nanofiller such as graphene nanoplatelets and hyperbranched polymer nanoparticles.

Keywords: fracture mechanisms, epoxy adhesives, filled epoxy resins, inorganic fillers, nanocomposites, hyperbranched polymer fillers

1. Introduction

Epoxy resins are among the most commonly used polymeric materials in structural applications, such as adhesives and fiber-reinforced composites. Moreover, they are widely employed in other nonstructural applications, i.e., as a coating in electronic and textile industries due to their great thermal, electronic, and mechanical properties [1, 2].

Although their wide use in the cited fields, highly cross-linked epoxy resins are rigid and brittle in nature and lose much of their structural integrity when damaged, thus limiting their use as structural materials (adhesives and composites).

In the last three decades, also due to the successful development of nano- and microparticles with different shapes, dimensions, and chemical features, nano-/microparticles have been

extensively studied as effective tougheners to overcome the natural fragility of epoxy resins. As reported by Kinloch [3], the addition of 15–20 vol% fractions of dispersed rubbery particles (diameter of $\sim 0.5\text{--}2\ \mu\text{m}$) can lead to an increase of the strain energy release rate G_{IC} by a factor of 10–15. Quan et al. [4] have increased the DGEBA epoxy resin fracture energy from $343\ \text{J/m}^2$ for the neat matrix to $2671\ \text{J/m}^2$ for epoxy modified by 30 vol% of core-shell rubber particles. Carbon nanotubes are also used as tougheners in epoxy resin and, according to the work by Gojny et al. [5], a nanotube content of only 1 wt% increases the critical stress intensity factor K_{IC} from 0.65 to $0.82\ \text{MPa m}^{1/2}$. Zotti et al. [6] report an increase of the G_{IC} value of about 350% with the addition of metallic iron core-inorganic shell nanoparticles (0.2 wt%). Ternary systems are extensively used in order to exploit the synergistic effect of the single elements on the fracture toughness; this is explained by Wang et al. [7], who have obtained an increase of about 108% in K_{IC} using a rubber/graphene/epoxy system.

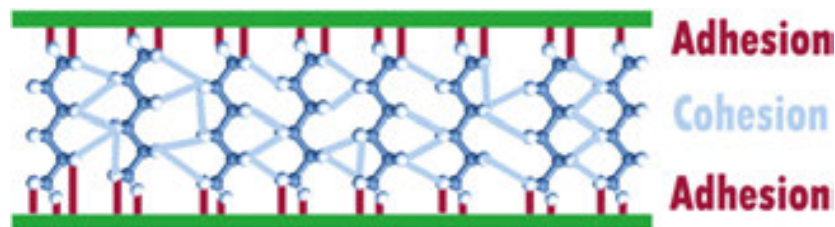


Figure 1. Comparison between cohesion and adhesion in an adhesive joint.

In an adhesive two main forces could be distinguished, i.e., cohesive and adhesive forces. The first could be considered as the inherent strength of the material related only to the chemical nature in terms of morphology and chemical structure. The second defines the complex interaction system between the adhesive and substrate therefore strongly affected by the contact surface morphology. **Figure 1** shows the difference between cohesive and adhesive forces.

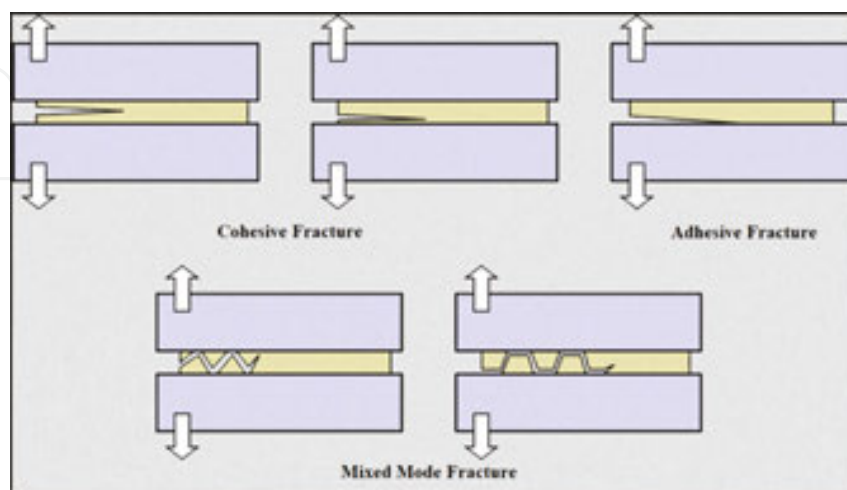


Figure 2. Adhesive joint fracture mode illustration.

Two adherent surfaces can fail according different fracture types (see **Figure 2**):

1. Cohesive fracture: the fracture propagates through the bulk resin that constitutes the adhesive layer. The fractured adhesive will cover both adherent surfaces. This kind of fracture generally occurs when the adhesion strength is stronger than the cohesion one.
2. Adhesive fracture: the fracture propagates through the adherent/adhesive surface. Only one of the adherent surfaces will be covered with the adhesive. This kind of fracture generally occurs when the adhesion strength is weaker than the cohesion one.
3. Mixed mode fracture: the fracture jumps from one interface to the other. It is possible to observe traces of adhesive on both surfaces of the substrate.

In materials science, fracture toughness describes the ability of a material containing a crack to resist fracture, and is one of the most important properties of any material system for many design applications. There are two alternative approaches to fracture analysis: the energy criterion and the stress-intensity approach [8].

According to the energy approach, for brittle materials, the crack propagates when the available energy is higher than the energy needed to create two new fracture surfaces. For ductile materials also, other types of energy dissipation should be taken into account (such as plastic deformation) in the global energy balance to follow correctly the crack onset and growth. Based on the Griffith energy criterion, Irwin developed the present version of this approach [8]; for a linear elastic, it is possible to define the energy release rate G as the rate of change in potential energy with the crack area material. When a material fails a critical value of the energy release rate, $G = G_C$ can be defined as the measure of material fracture toughness [8]. According to the Irwin theory, assuming a loaded infinite plate containing a crack whose measure in length is $2a$ (**Figure 3**), the energy release rate is given by:

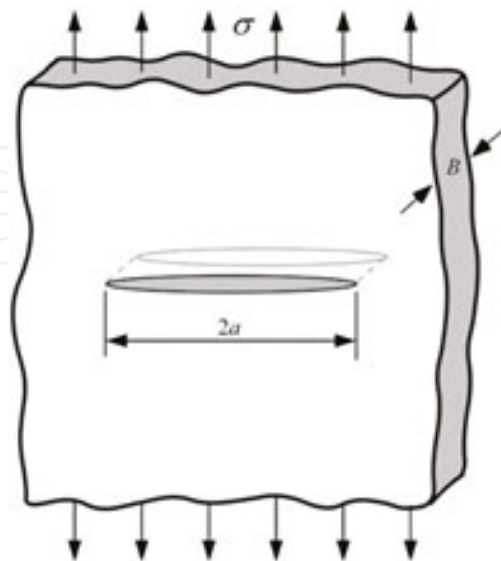


Figure 3. Through-thickness crack in an infinite plate subject to a remote tensile stress. In practical terms, “infinite” means that the width of the plate is $\gg 2a$ [8].

$$G = \frac{\pi\sigma^2 a}{E} \tag{1}$$

where E is Young’s modulus, σ is the remotely applied stress, and a is the half-crack length.

Since, $G = G_C$ when the crack starts to propagate, the relation between stress and crack size for failure can be expressed as:

$$G_C = \frac{\pi\sigma_f^2 a}{E} \tag{2}$$

Considering an elastic material, each stress component of an elemental unit near the tip of the crack can be written as reported in **Figure 4**. It is interesting to note that in each equation, a proportional factor K_I , called stress intensity factor, appears. Knowing the value for this parameter, the entire stress state near the crack tip can be defined. Similar to the energy approach, failure occurs in correspondence to a critical stress intensity factor, $K_I = K_{IC}$. K_{IC} is an alternate measure of fracture toughness, and in the case depicted in **Figure 3**, the stress intensity factor can be written as follows:

$$K_I = \sigma\sqrt{\pi a} \tag{3}$$

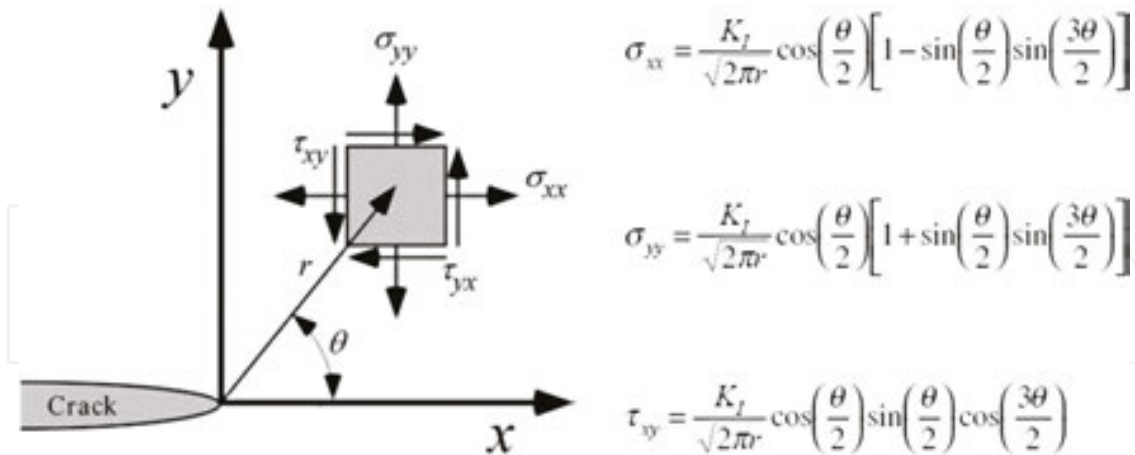


Figure 4. Stresses near the tip of a crack in an elastic material [8].

Failure occurs when $K_I = K_{IC}$. In this case, K_I is the driving force for fracture and K_{IC} is a measure of material resistance. As with G_C , the property of similitude should apply to K_{IC} . That is, K_{IC} is assumed to be a size-independent material property [8].

The comparison of Eqs. (1) and (3) results in a relationship between K_I and G :

$$G = \frac{K_I^2}{E} \quad (4)$$

This same relationship obviously holds for G_C and K_{IC} . Thus, the energy and stress-intensity approaches to fracture mechanics are essentially equivalent for linear elastic materials [8]. As previously stated, epoxy resins are brittle in nature, and in order to improve the cohesive fracture toughness, a second nano-/microphase is generally added. The fracture behavior of toughened polymers may involve several mechanisms, each one contributing toward the total fracture toughness of the material [9].

The chapter aims to describe the different mechanisms that cause the epoxy adhesive fracture toughening, with special attention to the correlation between fracture surface morphology and fracture toughening mechanisms. The chapter is divided into two main parts: (i) an overview on the possible fracture toughening mechanisms that may occur in epoxy adhesives and (ii) a study of toughened epoxy adhesives based on the filler nature.

2. Epoxy resins and failure modes

The epoxy group, when bonded chemically with other molecules, forms a large three-dimensional network. The process by which chemical bonding is achieved is called curing, where the fluid resin changes to a solid form. Among curing agents, various amines [10], anhydrides [11] and Lewis acids [12] are employed to cure the epoxies. The properties of the resulting epoxide resins (**Figure 5**) depend upon the epoxy, the curing agent, and the curing process. For example, when curing agents such as aromatic amines [13], acid anhydrides [14], and BF_3MEA [15] are used with proper epoxy resins and fully cured, the epoxies attain high glass transition temperature (T_g) and are thus suitable for high-temperature applications.

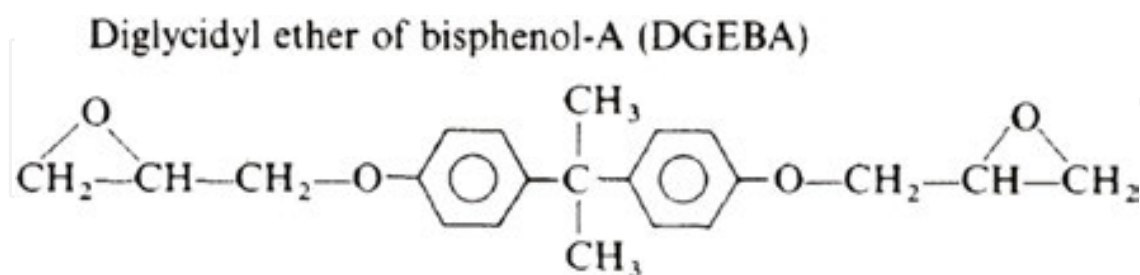


Figure 5. Chemical structure of DGEBA, an epoxy resin [16].

The cure process of an epoxy resin leads to the formation of a network consisting of epoxy molecules cross-linked to the reactive groups of the curing agent following the chemical stoichiometry of the compound. The mechanical properties of the cured resin are strictly dependent on the level of cross-linking achieved during the processing stage; in fact, a lower cross-link density will reduce the glass transition temperature and the storage modulus

improving the fracture toughness allowing greater elongation before failure. In the case of fully cross-linked system, the higher complexity of the formed network structure will induce an increase of the T_g with a lowering of the maximum deformation allowed before failure.

The topic of improving the mechanical properties of polymers by the addition of second-phase fillers has received a great attention in the scientific and industrial community throughout the last few decades [16]. Rubber and inorganic particles are the two main classes of fillers used to increase the fracture toughness of epoxy resins. Over the decades, starting from these two classes, new filler typologies were developed, and very recently nanomodification has become a suitable tool to optimize properties of polymers by designing their structure at a nanoscale. That has led to considerable improvements of mechanical properties of polymers, especially in terms of stiffness, strength, and toughness [17, 18].

The fracture behavior of toughened polymers may involve several mechanisms, each one contributing toward the total fracture toughness of the material. Such possible mechanisms are schematically depicted in **Figures 6** and **7**, and are the following: (1) shear band formation, (2) fracture of rubber particles, (3) stretching, (4) debonding and (5) tearing of rubber particles, (6) transparticle fracture, (7) debonding of hard particles, (8) crack deflection by hard particles, (9) cavitated or voided rubber particles, (10) crazing, (11) craze tip plastic deformation, (12) diffuse shear yielding, and (13) shear band/craze interaction (**Figure 6**).

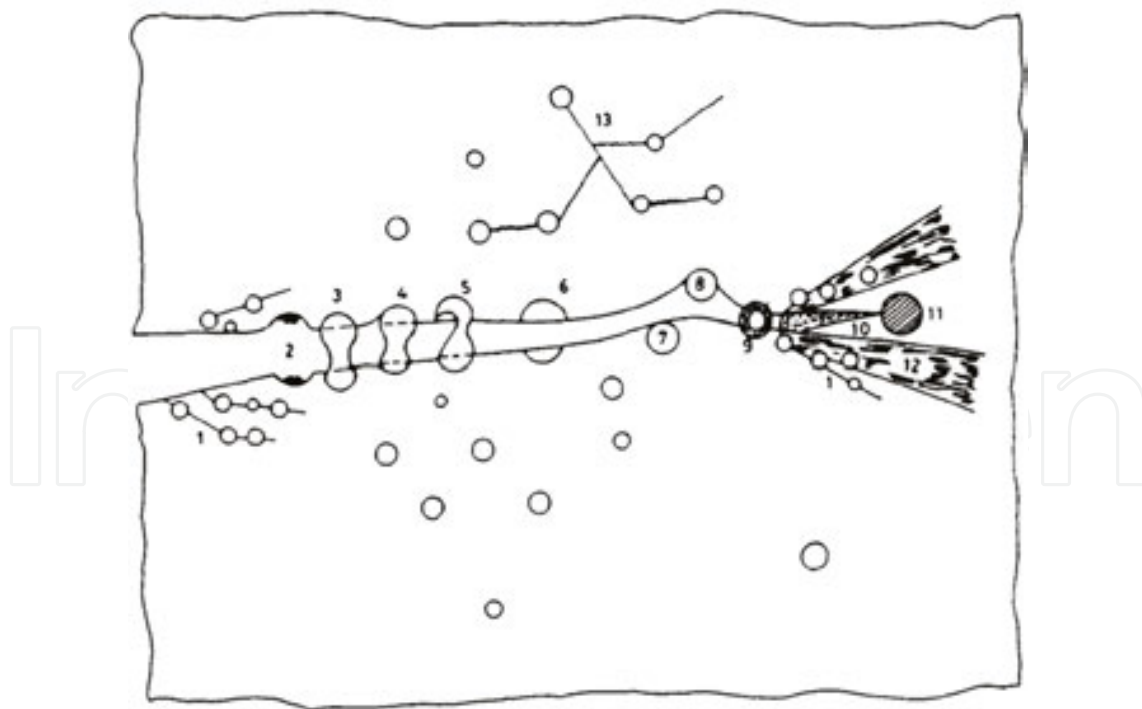


Figure 6. Toughening mechanisms in particle filled epoxy adhesive: (1) shear band formation, (2) fracture of rubber particles, (3) stretching, (4) debonding and (5) tearing of rubber particles, (6) transparticle fracture, (7) debonding of hard particles, (8) crack deflection by hard particles, (9) cavitated rubber particles, (10) crazing, (11) craze tip plastic deformation, (12) diffuse shear yielding, and (13) shear band/craze interaction [19].

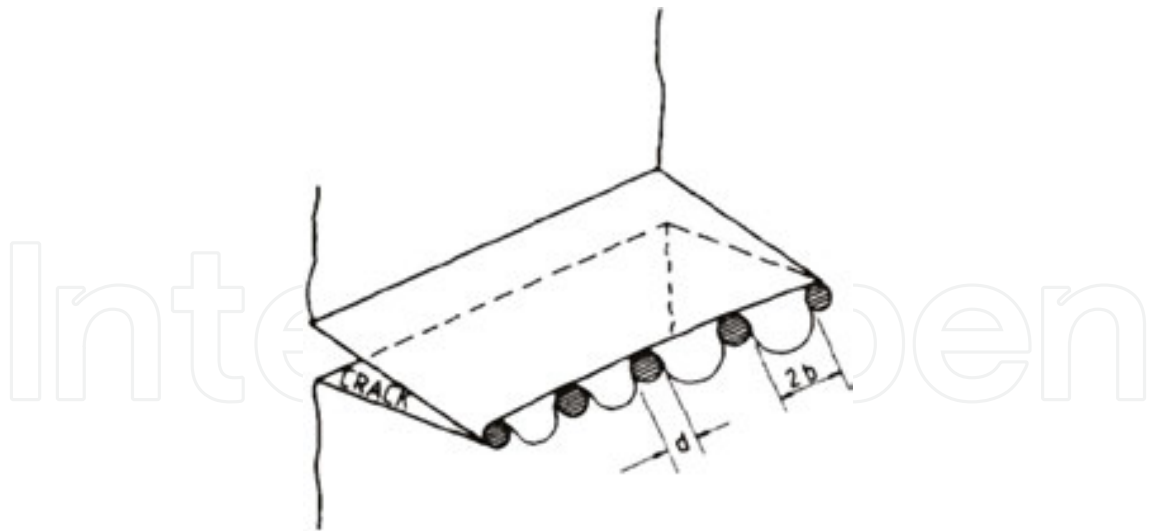


Figure 7. Crack pinning mechanism. The bowed crack front is at the verge of breaking away from pinning [19].

Energy dissipation mechanisms can occur in a toughened polymer at the same time, depending upon the nature of particles and matrix. The modeling of absorbed energy associated with each mechanism represents an important issue in the designing as well as in the verification stage. The main relationship reported in the current literature is reported below.

2.1. Rubber particle mechanisms: stretching, tearing, and debonding

Kunz-Douglass et al. [20] have developed a simplified model to estimate the energy dissipation (ΔG_{IC}) associated with the stretching, tearing, and debonding of rubber particles. According to this approach, rubber particles store elastic energy, equal to ΔG_{IC} , which is irreversibly dissipated (e.g., as heat) when the particle fails either by debonding from the matrix or by tearing, and is given by:

$$\Delta G_{IC} = 4\gamma V_p \left[1 - \frac{6}{(\lambda^2 + \lambda + 4)} \right] \quad (5)$$

where γ is either the specific energy of interface required to debond rubber or the rubber tearing energy, V_p is the rubber particles volume fraction, and λ is either the extension ratio at the time of debonding or rubber tearing.

2.2. Transparticle fracture

Considering an elastic particle of mean radius r , its specific fracture energy γ_p is given by:

$$\gamma_p = \frac{2r}{E} \eta^2 \sigma_f^2 \quad (6)$$

where η is the stress concentration factor at the particle equator and σ_f is the fracture stress. Considering that the number of particles N of mean radius r , per unit area of surface is:

$$N = \frac{3}{2} \frac{V_p}{\pi r^2} \quad (7)$$

Thus, the increase in toughness due to the fracture of particles is:

$$\Delta G_{IC} = 3\eta^2 r E V_p \varepsilon_f^2 \quad (8)$$

where $\varepsilon_f (= \sigma_f/E)$ is the fracture strain of the particle. For a uniaxial stress field $\eta = 2$.

2.3. Crack deflection

The crack is diverted by the particle, resulting in an increase of the crack surface area. This causes an increase in fracture energy given by:

$$\Delta G_{IC} = \frac{3\gamma_m V_p}{2} \quad (9)$$

where γ_m is the matrix specific fracture energy. According to this equation, the crack deviation leads to an increase in the fracture surface area, which is equivalent to half the surface area of the particle (i.e., $2\pi r^2$) minus the matrix area in absence of the particle (i.e., πr^2). Generally, the crack does not propagate along the whole particle surface, and then the deviation may be less. Consequently, Eq. (9) could overestimate the fracture toughness increase.

Deflection of cracks is commonly distinguished into:

1. Tilting: in-plane deflection, resulting in a mixed-mode (I/II) crack tip stress state.
2. Twisting: out-of-plane deflection, resulting in a mixed-mode (I/III) crack tip stress state.

Slender rods or fibers with high aspect ratios are more effective than disc-shaped particles or spheres in deflecting and twisting the propagating crack and hence in toughening [21, 22].

2.4. Crack-pinning

The obstacles (hard filler particles) create the obstruction to the propagation of the crack front and cause an increase in toughness by bowing out the crack front between the particles (**Figure 7**). Lange [23] has given a relation for the increase in fracture energy due to pinning as:

$$\Delta G_{IC} = \frac{T}{2b} \quad (10)$$

where, T is the line energy of the crack front and $2b$ is the interparticle spacing. The interparticle spacing can be obtained from:

$$b = d \frac{(1-V_p)}{3V_p} \quad (11)$$

where $d = 2r$. For a penny-shaped crack [24], Lange showed that the line energy is:

$$T = \frac{2r}{3} \gamma_m \quad (12)$$

Thus,

$$\Delta G_{IC} = \frac{r\gamma_m}{3b} \quad (13)$$

This equation predicts a linear relationship between the increase in fracture energy and the ratio r/b . However, this is not observed in practice except in the case of a glass-filled alumina [25].

The increase in G_{IC} required to bow out the crack front was then calculated by Evans assuming that the derivative of strain energy with respect to the interparticle spacing is equal to the increase in toughness. This model was confirmed by the experimental results of Moloney et al. [26] relative to epoxy resin filled with alumina and silica particles at low volume fractions. The agreement between theory and experimental results fails when high volume fractions are considered, likely because the theory assumes a semicircular "bow" crack front, while in these conditions it is semielliptical [26].

2.5. Crack tip yielding

The cited mechanisms can induce yielding and flow of the polymer near the crack tip. This effect hinders the crack propagation phenomenon, increasing the fracture toughness of the resin. It is well known that a polymer is characterized by covalent bonding along the polymeric chains, but chains can interact among themselves through weak van der Waals forces. When a local stress is able to overcome these forces, a narrow gap is formed. This forming gap, called craze, is not able to grow further, because it is held together by the covalent bonding of the

chains. Crazes scatter the light due to their microscopic dimensions. The polymeric chains that bridge the craze are grouped to form fine filaments called fibrils, visible only with an electron microscope (see **Figure 8**).

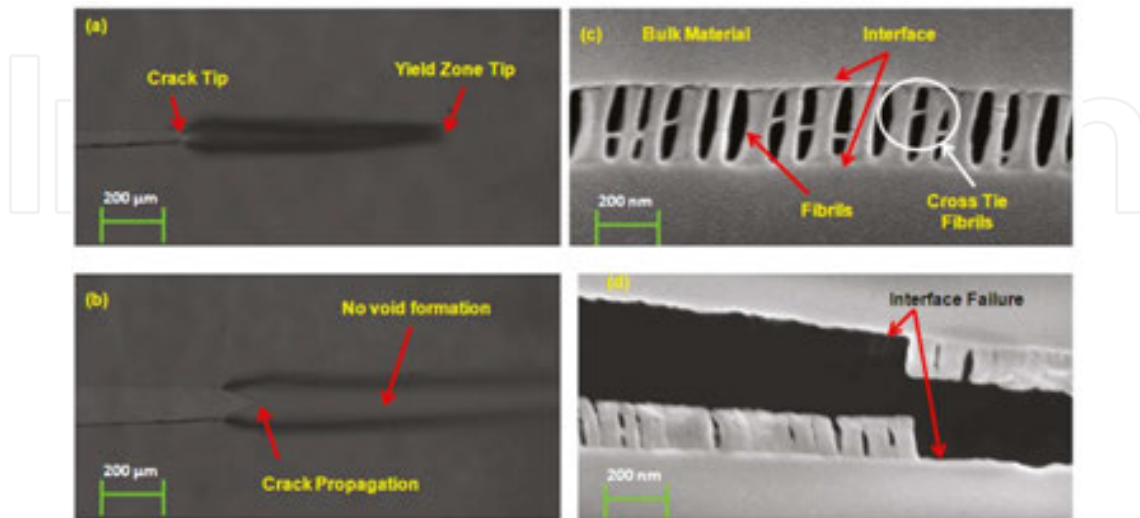


Figure 8. Shear yielding in 0.5 mm thick sheet of polycarbonate (a) before crack propagation, (b) after crack propagation and crazing in 800 nm thick polystyrene film, (c) fibril formation, and (d) fibril breakage [27].

3. Toughening mechanisms in modified epoxy adhesives

All possible failure mechanisms for filled polymer, has been reported in Section 2. Which of the cited mechanisms occur in the polymer depends on different factors: filler nature, matrix typology, curing agent, temperature, and load rate [19]. In the following paragraphs, the plausible mechanisms that can occur in epoxy adhesives filled with different typologies of filler are reported and discussed.

3.1. Rubber-toughened epoxies

The toughening of thermoplastics by rubber has been in existence for over 70 years but the addition of rubber to thermoset resins (epoxies) is only about 45 years old. The work by Sultan et al. [28] showed that worthwhile improvements could be effected by adding certain liquid rubbers to epoxide formulations.

Carboxyl-terminated butadiene-acrylonitrile rubber (CTBN) (**Figure 9**) is widely employed as a toughening agent in epoxy adhesives because it satisfies both the requirements needed to maximize the toughening effect [19, 29, 30]. The first requirement is the compatibility with the matrix, i.e., the liquid rubber must be soluble in the uncured matrix, but must precipitate out during the curing process. The second requirement is the reactivity between epoxy group and rubber chains.

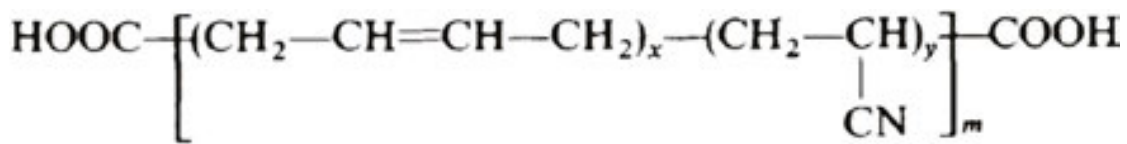


Figure 9. Chemical formula of CTBN rubber [19].

The addition of rubber to a brittle resin modifies its various characteristics. For example, it causes a reduction in stiffness, lowers T_g , plasticizes the matrix, reduces the yield strength, and increases the linear thermal expansion coefficient [31]. However, it also significantly increases the fracture resistance [32]. Because of such a gain in toughness, rubber-toughened epoxies are being used for various engineering applications.

Generally, the fracture energy, G_{IC} increases with increasing elastomer concentration up to about 16–17% and then decreases (Figure 10). Such behavior is seen because of the change of the elastomer from a dispersion phase to a blend at high CTBN concentration. Using this filler typology, the maximum fracture energy of the rubber-modified epoxy can also be 30 times that of the unmodified epoxy [33].

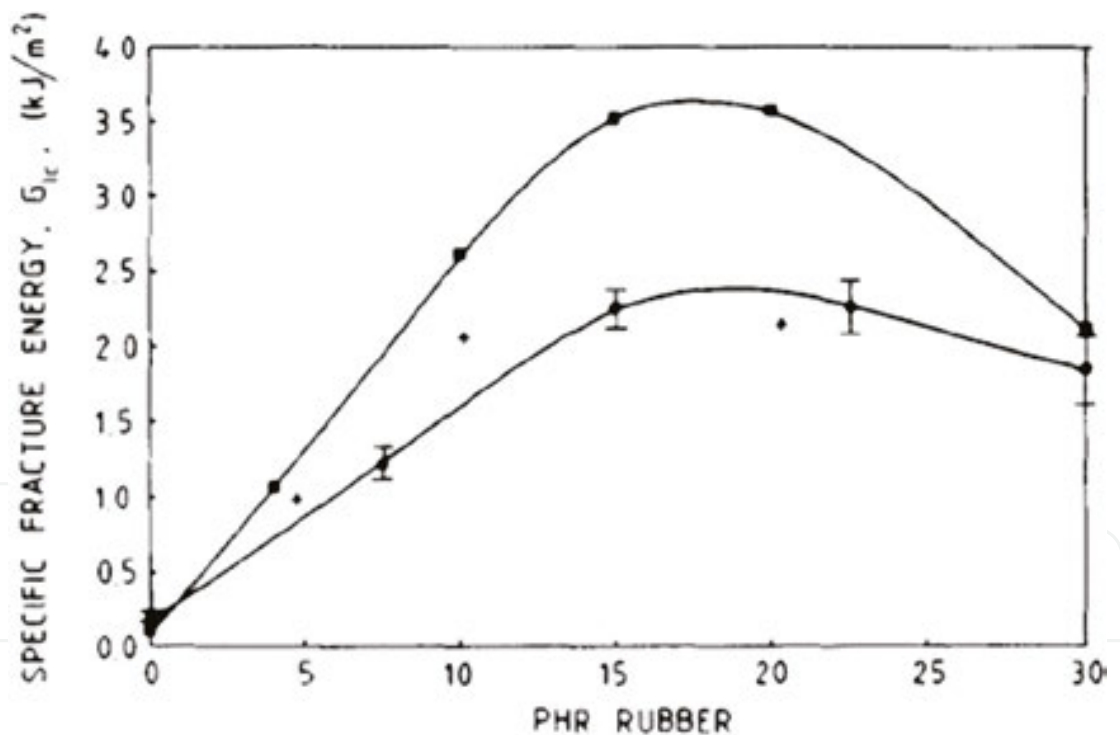


Figure 10. Variation of specific fracture energy, G_{IC} with rubber content. Different symbols are relative to different works [19].

Besides the reactive rubbers, several insoluble, unreactive rubber modifiers, such as core-shell rubbers (CSR) and dispersed acrylic rubbers (DAR) were used to modify the epoxy systems [34]. Dispersion of epoxy insoluble rubbers has resulted particularly useful in many adhesive and composite applications as the dispersed phase volume is not remarkably affected by curing

condition variations [35], and above a certain level of content, CTBN rubbers do not affect glass transition temperature of the final system. Moreover, the modulus of these modified epoxy systems can be varied independently of T_g .

Many theories have been proposed to explain the toughening mechanisms occurring in rubber-filled epoxy resins mainly based on the mechanisms identified in rubber-toughened thermoplastics. These theories involve deformation mechanisms such as shear yielding, crazing, and interaction among crazes and shear bands to explain toughening effect. According to these theories, rubber particles are considered initiation sites for crazes and shear bands and they also act as obstructions for the growing crack, reducing the intrinsic flaw size. The effect of rubber particles on crazes and crack propagation leading to reduced flaw size implies an increase in fracture toughness of the final system [10, 36].

The remarkable increase in volume during tensile creep tests on rubber-filled epoxy resins suggests the occurrence of a massive crazing of the specimen. It is noteworthy that this approach is verified for thermoplastic materials, but other contributions are to be considered to explain the toughening mechanisms in epoxide resins.

Stretching and tearing of the rubber particles can be considered as a different toughening mechanism. This mechanism is proposed by Kunz-Douglass et al. [20] by following the propagation of a crack using an optical microscope, have found that stretching and tearing of particles could be considered as the major source of energy absorption also in toughened epoxies. In their model, contribution of shear yielding to the fracture toughening was completely ignored as they did not notice this contribution neither in unmodified or modified epoxy.

Detailed microscopic analysis of the stress whitening region in fractured rubber-toughened epoxy resin showed that shear yielding cannot be totally neglected. In fact, these surfaces appear to be characterized by many small holes larger than the original particle size and yielding of the matrix (observed as tear marking) near the particles. The holes are the consequence of the dilatation of the original rubber particles, while the shear yielding is caused by the intense tri-axial stress state around the particles, which induce a noteworthy deformation into the matrix.

A similar model was proposed by Yee and Pearson [37], to account for the increased toughness of the rubber-filled epoxies. According these authors, the large dissipation of energy near the crack tip is responsible for the increased crack growth resistance and this deformation involves mainly two processes: (1) the cavitation in the rubber particles and in the surrounding matrix and (2) the plastic shear yielding in the epoxy matrix. According to this model, shear yielding is one of the main source of energy absorption for rubber-toughened epoxy resin, which causes a significant tip deformation that induce a remarkably reduction of the local stress concentration enhancing the fracture toughness of the final system.

Another remarkable mechanism in rubber-modified epoxy resins is the voiding. The presence of the rubber particles ahead the crack tip induces a tri-axial stress field when tensile load is applied to a notched specimen that causes a high hydrostatic tension around particles. The consequent dilatation promotes their cavitation and the enlargement of the resultant voids

(Figure 11). These voids formed are further enhanced by thermal stresses induced during the cooling from the curing to ambient temperature.

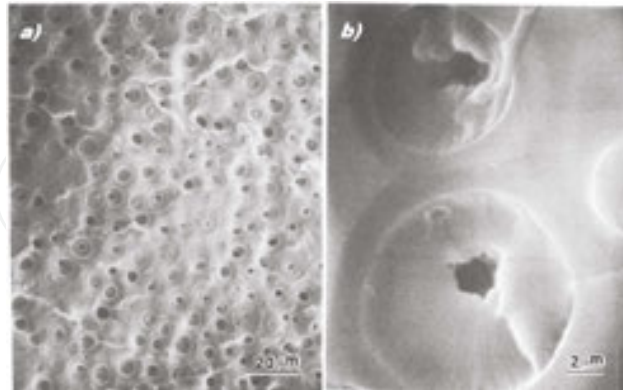


Figure 11. Fracture surface of a rubber-toughened epoxy resin: (a) low and (b) high magnification [38].

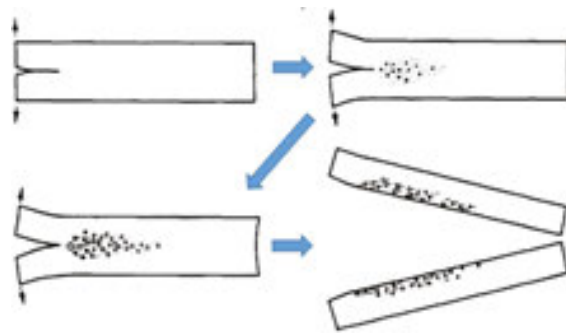


Figure 12. Schematic representation of the deformation processes ahead of a crack tip [37].

In the work by Yee et al. [37] two epoxide resin systems toughened with CTBN elastomers were studied by uniaxial tensile dilatometry to investigate the involved fracture mechanisms. Results have shown that the presence of the rubber particles has a twofold effect: (1) inducing shear flow at lower strain rates and (2) promoting cavitation at higher strain rates. In both cases, there is the formation of a shear yielded region ahead the crack tip, which hints the crack propagation. By analyzing tensile dilatometry results, it was showed that the formation of a region characterized by voids and shear bands ahead the crack tip occurs. This region blunts the crack and this implies that the crack tip behaves as it was larger than reality, increasing the fracture toughness level. On increasing the load, voids continue to grow and the region characterized by shear band extends its dimensions. Moreover, the crack propagating through the voided plane increases the fracture path, and then the energy is dissipated. The fracture process described above is schematically depicted in Figure 12. As shown in Figure 11, the matrix surrounding the voids exhibits a notable plastic deformation as evidenced by the beveled edges of the voids. The plastic deformation becomes larger as the particle-particle distance decreases; this is an evidence for particle-particle interaction.

The interaction between particles can also be seen by comparing the diameters of the fracture surface cavities (SEM) with the diameters of the undeformed rubber particles at various levels of rubber content. It appears clear that many cavities are larger than the corresponding rubber particles with the same filler content, indicating a strong interaction among near particles. At high rubber content, the expansion in the diameter from the undeformed to the fracture cavity becomes more relevant due to the increase of the particle interaction [38].

The critical strain-energy release rate, G_{IC} , is plotted against the rubber content for three rubber-toughened epoxies as given in **Figure 13**. These results show that fracture toughness is a strong function of rubber content, but not significantly dependent on the rubber particle size. The Hycar CTBN 1300X8 modified epoxies (828-8), containing $\sim 1 \mu\text{m}$ diameter rubber particles, are not significantly tougher than the Hycar CTBN 1300X15 modified epoxies (828-15), which have $\sim 5\text{--}10 \mu\text{m}$ diameter rubber particles [37].

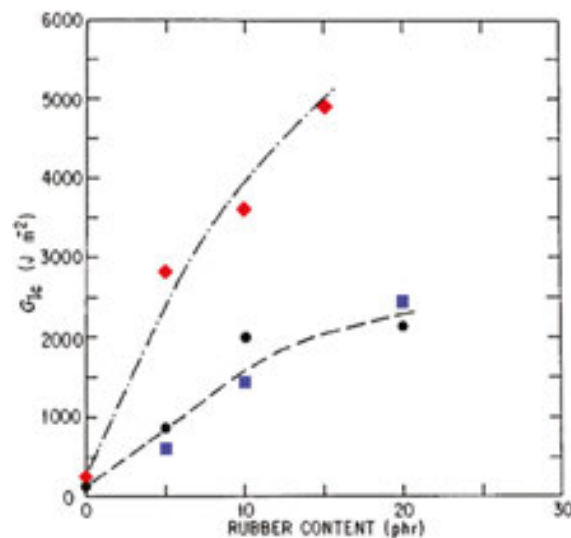


Figure 13. The strain-energy release rate G_{IC} as functions of rubber content, for three types of modifier: (●) 828-8, (■) 828-15, (◆) 828-BPA-8 [37].

In summary, in rubber-toughened epoxy resin, the main fracture mechanism recognized are the following: shear band formation near rubber particles, fracture of rubber particles after cavitation, stretching, debonding and tearing of rubber particles, voiding, crazing, diffuse shear yielding, and shear band/craze interaction.

3.2. Particle-filled epoxies

Over the decades, besides using rubber as a toughening agent for polymers, several inorganic fillers such as alumina [39], silica [40], glass beads [41], and aluminum hydroxide [42] have been considered. Generally, the preparation of inorganic particle-filled resins is relatively simple: filler and resin are mixed and cured, imposing vacuum before the cure process to allow the spilling out of the trapped air bubbles. To obtain polymers with high fracture toughness,

high modulus, and T_g rubber particles are often added to the inorganic particles/epoxy resin system [43, 44].

Inorganic particles are able to provide high physical and mechanical properties to the hosting matrix and therefore they could be an ideal candidate in the case of advanced engineering applications. These fillers have many advantages, such as low cost, reduce matrix shrinkage and polymerization heat during the cure process, and increase the elastic modulus, T_g and thermal conductivity [10, 23, 39, 40]. Also fracture toughness is affected by the presence of the particle filler: in fact it is generally higher than those of pure epoxy resin [40, 41]. The entity of the gain in mechanical properties depends on different factors: chemical nature of the filler, particle size, filler content, functionalization of the particles surface, and strain rate. Many works on fracture toughness of the particle-filled epoxy during fast [45–47] and slow [48] crack propagation have reported an increase of the K_{IC} value of the composite, together with an improvement in Young's modulus and yield stress (see **Table 1**).

| Volume fraction, V_p (%) | Mean particle size, d (μm) | K_{IC} ($\text{MPa m}^{1/2}$) | E (GPa) | σ_y (Mpa) |
|----------------------------|---|-----------------------------------|---------|------------------|
| 40 | 300 | 1.76 | – | – |
| | 160 | 1.74 | – | – |
| | 100 | 1.87 | – | – |
| | 60 | 1.83 | – | – |
| 0 | 100 | 0.60 | 3.5 | 100 |
| 20 | 100 | 1.30 | 6.1 | 108 |
| 30 | 100 | 1.62 | 7.7 | 121 |
| 40 | 100 | 1.87 | 9.8 | 133 |
| 50 | 100 | 2.21 | 12.5 | 150 |
| 40 (silane-treated) | 100 | 1.90 | – | – |

Table 1. Epoxy/silica composite with different filler content and surface treatment [19].

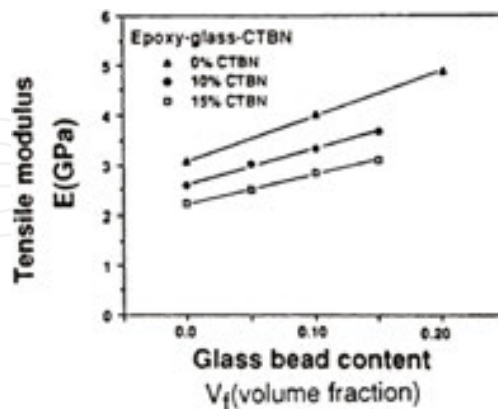


Figure 14. Tensile modulus as a function of glass bead content for different epoxy-CTBN compositions [44].

A simple and effective way to improve fracture energy without loss of strength and elastic modulus is to incorporate inorganic fillers in rubber-toughened epoxies. As reported in **Figure 14**, the presence of the CTBN rubber lowers the mechanical properties (tensile

modulus, E), but the addition of small amount of inorganic filler restore the modulus to the initial value. The G_{IC} value for the hybrid glass rubber-modified epoxy is much larger than for the glass-unmodified epoxy for a given temperature and volume fraction of glass [49].

It is well known that the presence of rigid (micro) fillers may induce several toughening mechanisms in epoxy matrices, for example, (1) crack deflection [21, 50], (2) plastic deformation [26, 51], and (3) crack front pinning [36, 52]. The first mechanism is always present, but minimally contributes to the total increase of fracture toughness in particulate-filled epoxy resins. Similar to rubber filled epoxy resins, the presence of inorganic particles induces a tri-axial stress state in matrix around it, promoting plastic deformation in the polymeric phase and then crack tip blunting. However, the main source of toughening in particulate-filled epoxy resins is the crack pinning.

This statement is supported by the work of Moloney et al. [26], in which the effect of alumina and silica particles on the fracture toughness of a filled epoxy resin was studied. It is noteworthy that in case of weak filler particles, such as aluminum hydroxide and dolomite [26], crack pinning cannot completely explain the fracture toughening, in fact, up to a certain filler content crack pinning is applicable, but over a critical content ($\sim 20\%$), the crack tends to propagate through particles, promoting a transparticle-fracture mechanism.

As reported by Kinloch et al. [36], who studied a hybrid system consisting of glass beads and rubber particles in an epoxy matrix, crack pinning is the main fracture toughness mechanism in systems operating at low temperature. Fracture can be described by the critical crack opening displacement criterion. At higher temperatures the crack pinning mechanism is overshadowed by the large plastic flow processes at the crack tip.

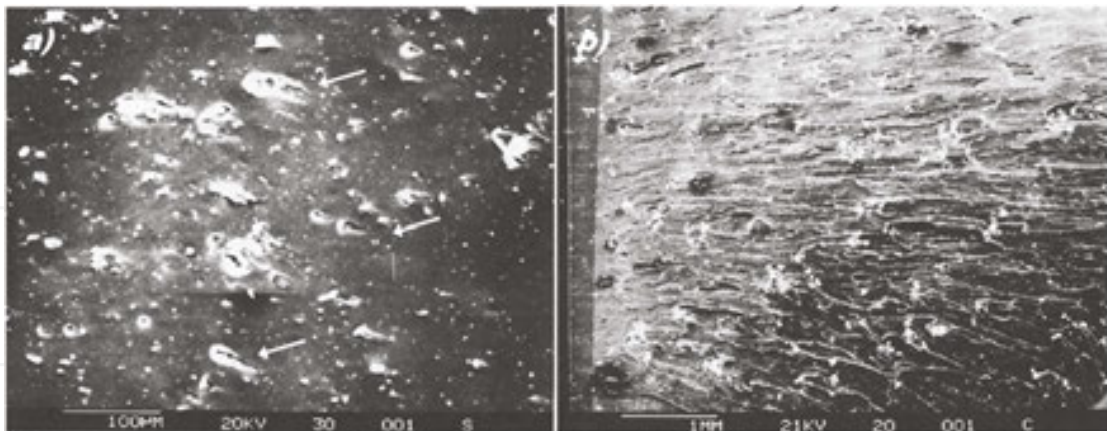


Figure 15. Fracture surfaces for (a) zirconia-epoxy showing crack pinning “tails” (white arrows) and (b) zirconia-rubber-epoxy showing crack initiations and arrests in stress whitened region [53].

The occurrence of crack pinning in zirconia epoxy and zirconia-rubber epoxy systems was also confirmed by the work of Low et al. [52], according to which crack pinning is the main fracture toughening mechanism in zirconia epoxy system, while in the hybrid resin there are evidence of cavitation and shear flow near the crack tip. Crack pinning is clearly indicated by the presence of the characteristic tails (white arrows) as given in **Figure 15**. **Figure 15(b)** shows the

hybrid system fracture surface, which is evident from the presence of many sites of crack initiation and arrest, with consequent remarkable fracture toughness increase (rubber particles debond/tear in correspondence of each initiation site, rising the dissipated energy).

Maxwell et al. [53] developed a hybrid glass-filled epoxy-polymer containing both rubbery and rigid particles. The values of G_{IC} for the unmodified and rubber-modified epoxy materials as a function of volume fraction of glass particles are shown in **Figure 16**. It is interesting to note that in systems without glass bead ($V_f = 0$), the value of G_{IC} continuously increases with the temperature, and in particular, in a rubber-modified system, the rise is of about an order of magnitude. At higher glass beads content, the G_{IC} levels up to a certain value and then decreases; this effect is more evident for the hybrid system. The optimum value of the filler content for the glass-epoxy system is about 0.3 with a G_{IC} increase of about 400%. Conversely, in the hybrid system, the optimum value is dependent on the temperature.

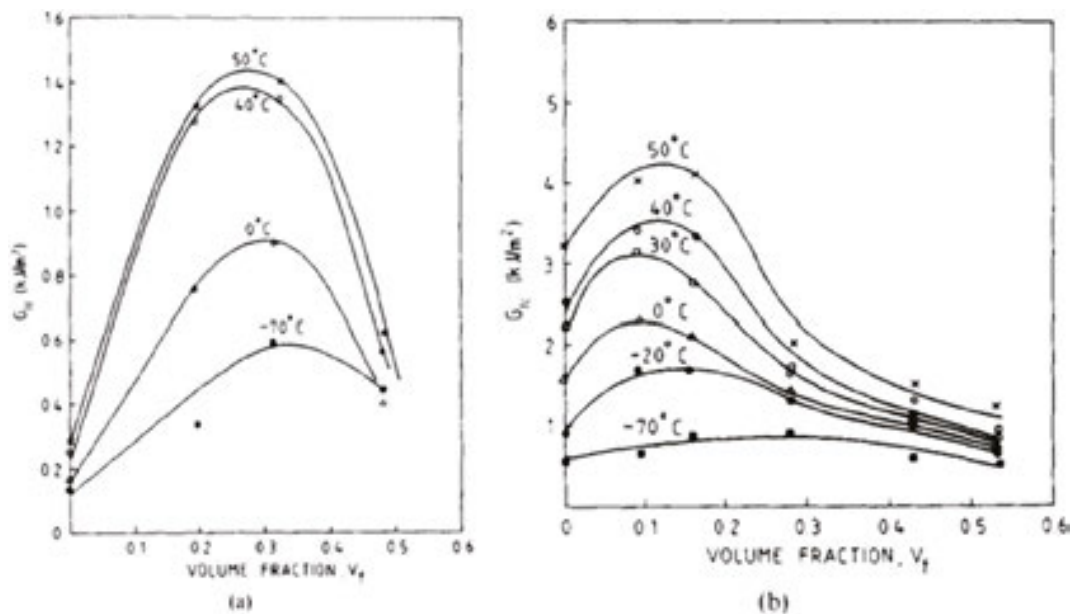


Figure 16. Fracture energy, G_{IC} , against volume fraction, V_f , of glass particles for (a) an unmodified epoxy and (b) a rubber-modified epoxy [49].

SEM observation can help to understand the fracture mechanisms that occur in a filled epoxy adhesive. A typical micrograph of a glass particle-filled resin is shown in **Figure 17(a)**, in which the tails behind the particles typically associated with the crack pinning mechanism are clearly visible. These tails are associated with the bifurcation of the crack front when it encounters the pinning position (i.e., the rigid particle) and to the subsequently meeting again of the two new crack fronts. **Figure 17(b)** shows the micrograph of the hybrid glass/rubber system. It is interesting to note the presence of many small holes, larger than the rubber particles, and a very rough surface, due to the massive shear flow during the crack propagation. The presence of few small tails behind the glass particles indicates a little contribution of the crack pinning to the global fracture toughening mechanism. However, the presence of few crack pinning characteristic tails in the hybrid system was predictable considering the curve of G_{IC} as a

function of glass bead content, in fact, the increase of G_{IC} for the presence of inorganic filler is very high (400%) in the rubber-free system, but is minimum (~40%) in the rubber toughened system.

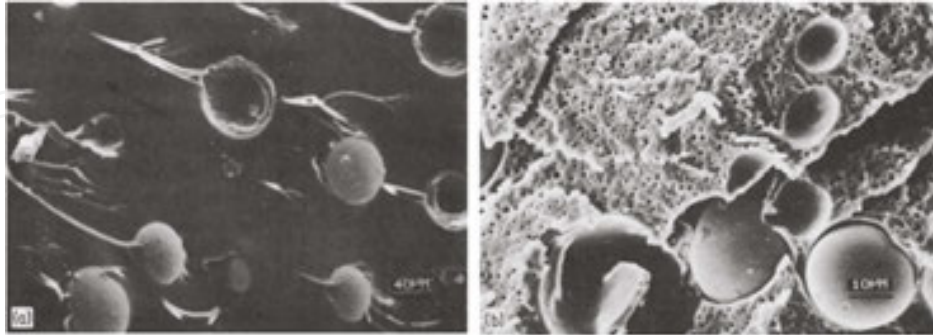


Figure 17. Scanning electron micrographs of fracture surfaces. (a) Glass particle filled unmodified epoxy (arrow indicates direction of crack growth). (b) Hybrid particulate-filled epoxy-polymer [19].

3.3. Thermoplastic-modified epoxies

Thermoplastic particles can be used as toughening agent in brittle epoxy resins, as they promote delocalized microcracking and crack bridging [54]. This typology of particles is extensively used to avoid a decline in modulus of the hosting matrix.

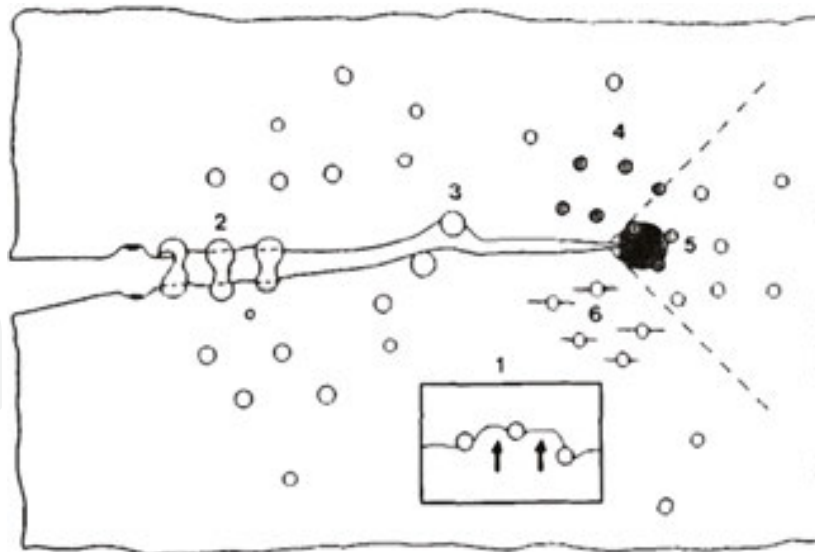


Figure 18. Schematic diagram of toughening mechanisms proposed for thermoplastic-modified epoxies: (1) crack pinning, (2) particle bridging, (3) crack path deflection, (4) particle yielding, (5) particle-yielding induced shear banding, and (6) microcracking [57].

Thermoplastic-modified epoxies are toughened by a mechanism called crack bridging (Figure 18) [55, 56]. The increase in K_{IC} observed in this toughened resin is due to the effect

of the rigid plastic particles that bridge the two crack surfaces limiting the opening of the crack tip. Crack bridging can also be explained considering that the energy is dissipated during the plastic deformation and consequent tearing of the plastic particles.

The effect of the crack bridging on the morphology of the fracture surfaces is simple to observe; generally, the surface of broken particles appears rich, yielded after a large plastic deformation.

Microscopic evidence for crack bridging can be seen in **Figure 19**, in which highly drawn particles of polyamide-12 [58] in the process zone ahead of the precrack are shown. It can be seen that the particles adhere well to the matrix and are capable of large plastic strains before failure. It is also apparent from the large deformations that the particles failed well after the crack had advanced through the matrix.

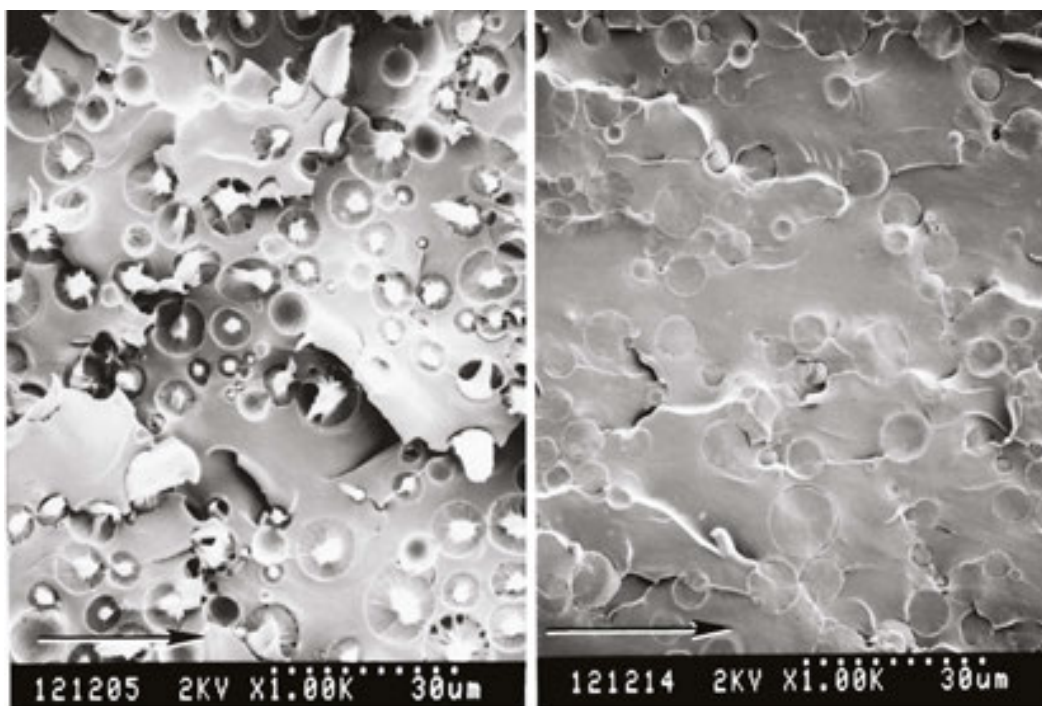


Figure 19. SEM micrograph showing the deformed polyamide-12 particles on the fracture surface a polyamide-12 modified epoxy from within the process zone (arrow indicates direction of crack propagation) [54].

Many works [57, 59] also mention the crack pinning as one of the mechanisms contributing to the fracture toughening effect of thermoplastic particles. These particles behave like impenetrable objects, similar to inorganic particulate filler previously cited. Indeed, the higher brittleness of the epoxy matrix compared to the ductile thermoplastic phase allows the consideration of these particles as relatively impenetrable.

Crack path deflection [58] is another cited mechanism responsible for the toughening of thermoplastic particle-filled epoxy resins. As described previously, in this mechanism, the particles cause the deviation of the crack front from the original path, increasing the fracture surface area and consequently the energy dissipation. Occurring of this toughening mechanism can be verified observing the fracture surfaces with SEM.

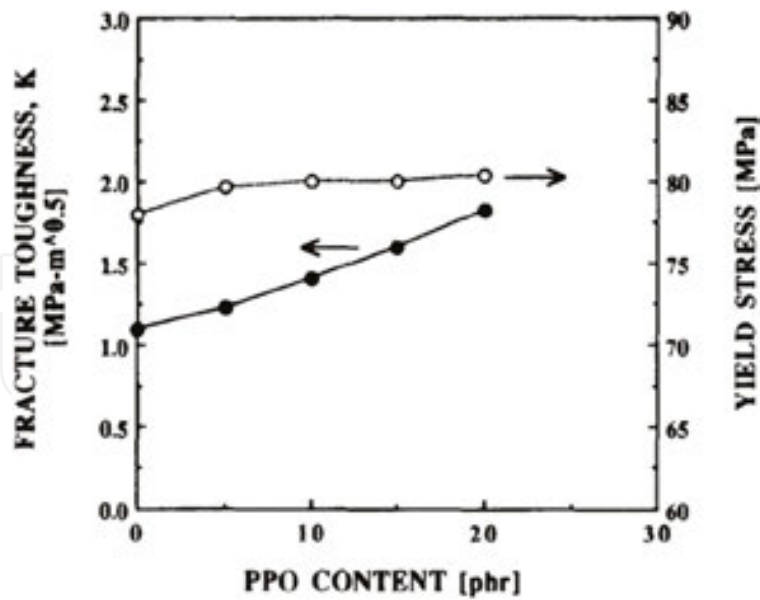


Figure 20. Fracture toughness increases with PPO content while the yield strength remains constant [54].

Thermoplastic particles also induce shear banding in the matrix, similar to rubber particles. In fact, during the yielding of the rigid particles, their modulus reduces up to that of the rubber, and this mismatch in modulus between matrix and yielded particles induces a remarkable stress concentration, initiating shear banding in the surrounding matrix. Pearson et al. [54] have modified an epoxy based on the diglycidyl ether of bisphenol A (DGEBA) with poly(phenylene oxide) (PPO). The fracture toughness of PPO-modified epoxies increases almost linearly with PPO content. These results are presented graphically in **Figure 20**. The simple linear relation between PPO content and fracture toughness is surprising since the morphology undergoes a dramatic change from a particulate morphology to the one that consists of continuous domains. Pearson et al. stated that the toughening mechanism is not massive shear banding as has been found for rubber-modified epoxies; instead, the PPO-modified epoxies are toughened by a microcracking mechanism and branching (**Figure 21**).

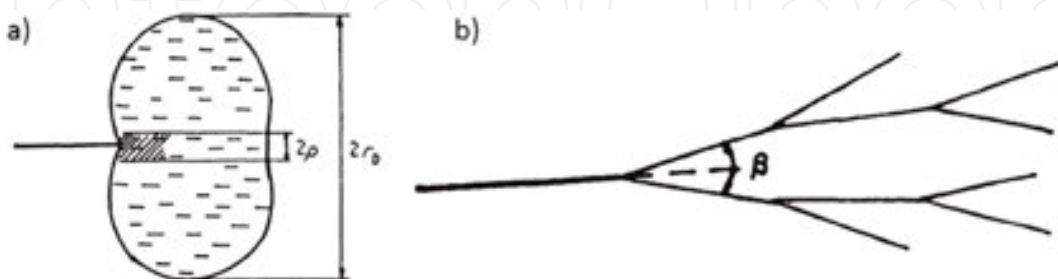


Figure 21. (a) Microcracking and (b) Branching mechanism at the crack tip [54].

According to Hodgkin et al. [60], the criteria for achieving good thermoplastic toughening could be listed as follows:

1. Thermoplastic backbone: this should have high thermal stability, should be soluble in the uncured epoxy, but must be phase separated during cure to form a multiphase morphology (as previously stated for the rubber particles).
2. Morphology: increase in optimum toughness is generally achieved through attainment of a cocontinuous or phase inverted morphology.
3. Reactive endgroups: it does not appear necessary to use functionalized endgroups in the toughening phase.
4. Cross-link amount: increasing the crosslinking density of the epoxy resins increases the efficiency of the toughening with thermoplastic particles (conversely to rubbers).
5. Molecular weight: high molecular weights of the employed thermoplastic filler promote the toughening of the matrix.

3.4. Layered nanofiller-modified epoxies

One of the most promising approaches to synthesize materials with barrier properties [61, 62], fire resistance [44], and increase of mechanical properties [10, 44] consists in dispersing an inorganic clay mineral in an organic polymer on a nanometer scale. Crack deflection is likely the major energy dissipation mechanism that occurs in nanoclay-filled polymers, where 1 nm thick clay platelets often tend to be stacked into microsized tactoids, readily able to perturb the growing crack front. Moreover, also debonding of nanoclay (often regarded as nanoclay delamination) and matrix shear banding contribute to the overall fracture toughness improvements [62].

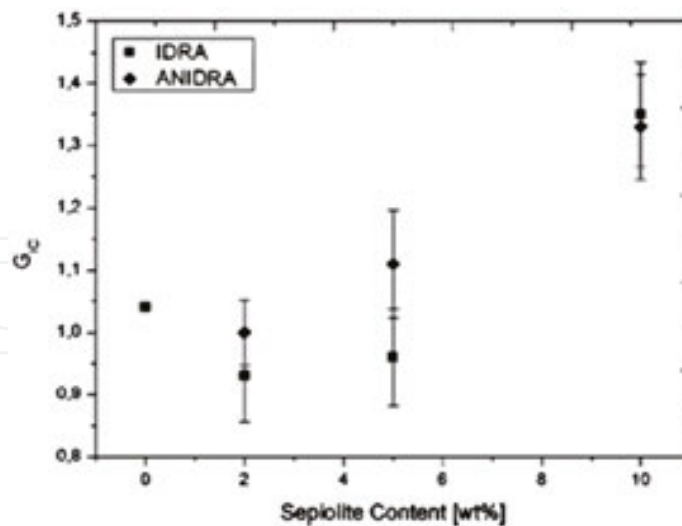


Figure 22. Critical strain energy release rate, G_{IC} , versus sepiolite content [10].

Evidence of the cited mechanisms can be seen in the work by Zotti et al. [10]. In this work the addition of sepiolite clay induces an increase of the strain energy release rate up to 30% (Figure 22). These authors pointed out that sepiolite clay particles might act as stress

concentration sites promoting clay-matrix debonding (orange arrow), which produces micro- and nanovoids and matrix shear yielding in the regions close to the crack tip (**Figure 23**). The high roughness of the fracture surface indicates the presence of a crack deflection mechanism.

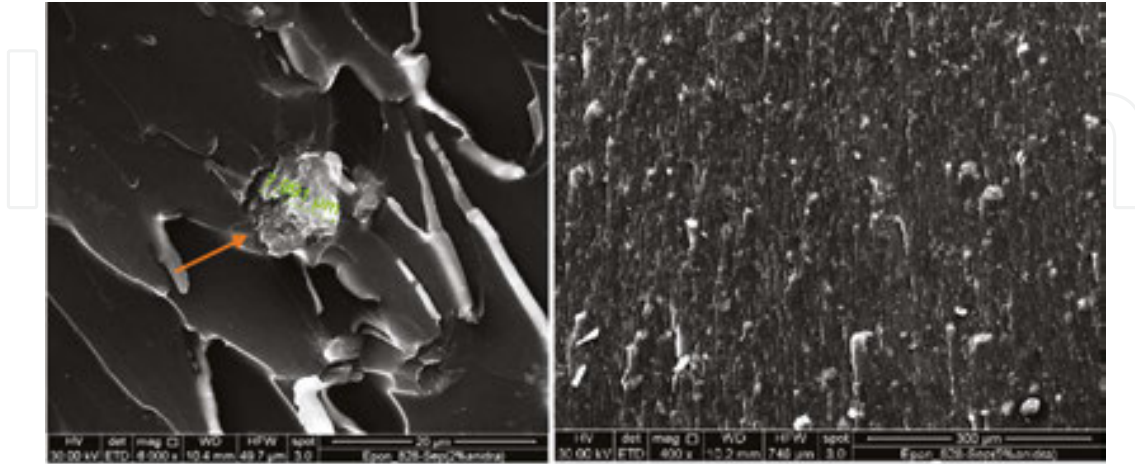


Figure 23. Fracture surface of a sepiolite/epoxy; (left) high and (right) low magnification [10].

To the group of the layered nanofiller belong graphene and its derivatives. This innovative material is constituted by a single sheet of sp^2 hybridized carbon atoms and therefore shows a honeycomb structure. This bidimensional structure shows excellent thermal and electrical conductivity, similar to carbon nanotubes (CNTs). Graphene also shares with CNTs a very high elastic modulus [55, 63]. Similar to clays, graphene is characterized by a layered structure, but owns higher mechanical properties thanks to the carbon backbone.

Graphene is able to remarkably increase the fracture toughness of an epoxy resin also with low content: in fact in the work of Raffiee et al. [56] a 65% increment in fracture toughness for 0.125 wt% of filler amount was reported. Fracture surface analysis indicates a doubled surface area for the graphene/epoxy system compared to the pure epoxy. This strong increase in the fracture surface area is indicative of a crack deflection mechanism. However, the fracture toughness contribution of this mechanism reduces increasing the filler content.

Chandrasekaran et al. [64] report similar observations in their work, where graphite nanoplatelets (GNPs) and thermally reduced graphene oxide (TRGO) were dispersed in epoxy matrix.

The fractured surface of graphene/epoxy nanocomposite, observable with SEM, shows higher roughness than the pure epoxy as presented in **Figure 24**. This again indicates that crack deflection is one of the toughening mechanisms in these nanocomposites. The difference between the two graphene types GNPs and TRGO is that, TRGO is produced via chemical exfoliation and hence contains some remnant oxide functionalities and a fewer number of layers. These factors improve the graphene dispersion in the epoxy matrix compared to the GNP/epoxy system. In fact, GNPs are prepared by metal intercalation of graphite and have less oxide functionalities and more number of layers compared with TRGO. The better

dispersion explains the higher surface roughness for the TRGO/epoxy composite when compared with GNP/epoxy (**Figure 24**).

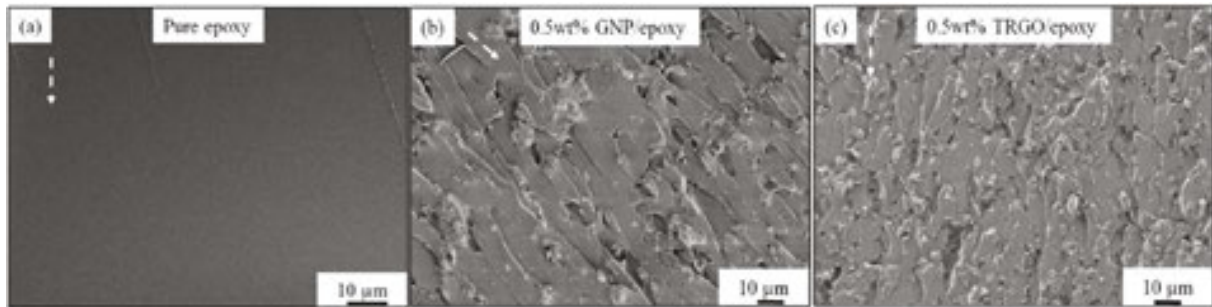


Figure 24. Increase in surface roughness of fracture surface (b and c) graphene/epoxy nanocomposite compared with (a) pure epoxy (white dotted line arrow indicate crack propagation direction) [65].

A 2D schematic of crack bifurcation and propagation at different heights showing the interaction of the crack front with the TRGO/GNP particle is shown in **Figure 25**. During the interaction between propagating crack front and graphene nanoplatelet there are two possible situations that can happen: (1) the crack front is deflected, taking a torturous path or (2) the crack front bifurcates around the platelet (**Figure 25a and b**) [65].

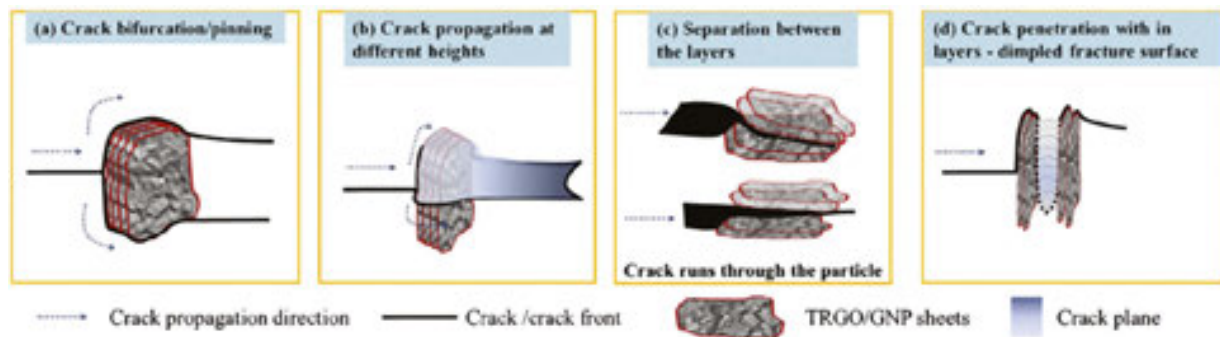


Figure 25. Schematic on the interaction of crack front with GNP/TRGO particles (white dotted line arrow indicates crack propagation direction): (a) crack bifurcation/pinning, (b) crack propagation at different heights, (c) separation between layers and (d) crack penetration with in layers - dimpled fracture surface [64, 65].

In **Figure 26**, the fracture surface of both the sides (for the ease of comparison, side B was electronically tilted by 180°) of the specimen is presented. A feature that was observed in the fracture surfaces is that there are places where there are no flow patterns as pointed out by the solid arrows in **Figure 26**. This fact indicates that this face is not the fracture surface of epoxy resin but the surface of TRGO/GNP particle. In this case, the crack runs along the surface of TRGO or GNP/epoxy interface. This failure mechanism occurs when the crack meets the edges of the graphene sheets. The crack continues to propagate in between the graphene sheets and finally passes through by separating the layers. Since the force between the sheets is a second-

dary force (van der Waals), the separation of sheets is facilitated with easy crack propagation (Figure 25c).

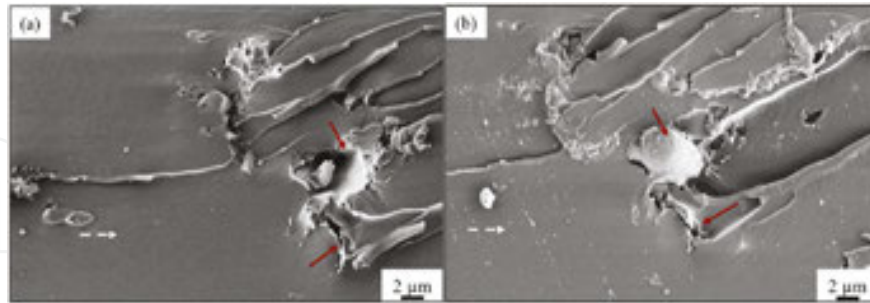


Figure 26. Scanning electron micrograph of both the sides of fracture surface for 0.1 wt% TRGO/epoxy (a) Side A and (b) Side B showing separation in-between the graphene layers that are oriented parallel and perpendicular to the propagating crack [64, 65].

Combination of crack deflection and separation between the graphene layers is another mechanism that can occur in graphene-toughened epoxy resins (Figure 24d). When the crack front is deflected by the graphene platelet, it goes around the particle until it meets the graphene edges. In some cases, the crack front can run between the graphene sheets, producing a characteristic “dimple type” fracture surface [65].

On increasing the graphene content, the surface roughness remarkably increases, as reported in Figure 27. It is interesting to note that at lower filler content (Figure 25a), bifurcation and pull-out are the main failure mechanisms. By increasing the filler weight percent, crack pinning and crack deflection became the predominant failure modes (Figure 25b and c). Finally, higher filler content promotes the separation between graphene sheets, reducing the surface roughness and consequently the K_{IC} value (Figure 25d).

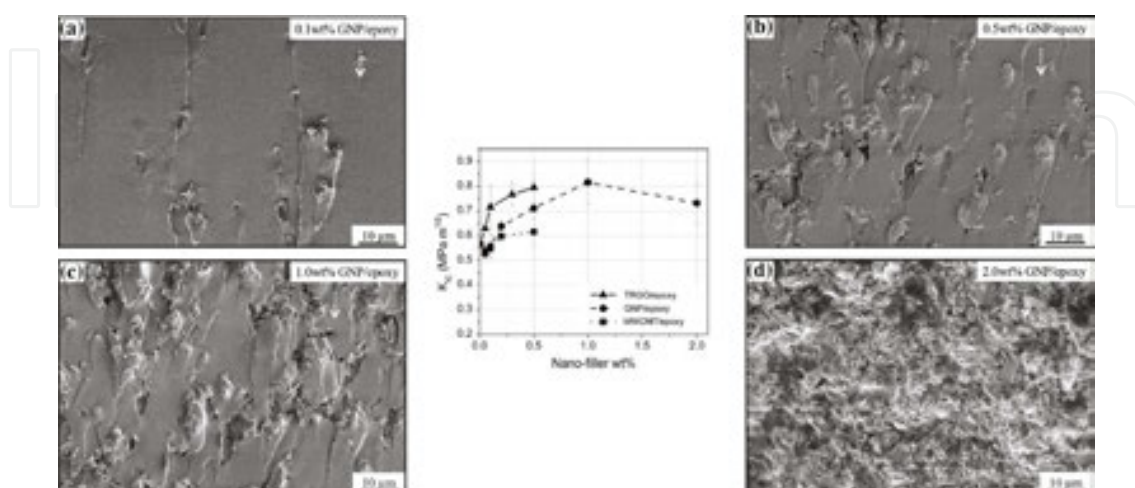


Figure 27. Fracture toughness as a function of weight percent of filler and corresponding SEM micrographs of the fracture surface of GNP/epoxy: (a) 0.1 wt%; (b) 0.5 wt%; (c) 1.0 wt%, and (d) 2.0 wt% [65].

3.5. Hyperbranched-modified epoxies

Hyperbranched polymers are characterized by different properties that stimulate their use as toughening agent in epoxy resins such as low melt and solution viscosities, large number of functional groups in the peripheral region, and small dimensions compared to polymer of equal molecular weight [66, 67]. Hyperbranched polymers have also been explored as novel, high potential, and low viscosity tougheners for epoxy resins that increase fracture toughness properties without deleterious effects on other properties [68].

SEM observations of fracture surface, performed by Fu et al. [69], showed cavitations at center and fibrous yielding phenomenon at edges, which indicated that the particle cavitations, shear yield deformation, and *in situ* toughness mechanism are the main toughening mechanisms. In this work, Fu et al. have synthesized an epoxy-terminated low viscosity liquid thermosetting aromatic polyester hyperbranched epoxy resin (named as HTTE) for the modification of DGEBA epoxy resins. The SEM of the XY plane (central region of the sample—**Figure 28a**) shows “sea-island” structures, “dimple-like” structures, and macroscopically sized stress-whitened zones surrounding the crack, which are generally the characteristics of rubber-modified epoxy resins and are called “toughness dimples.” The rubbery HBP particles cavitating generate voids, which scatter the light and induce the stress whitening phenomenon. As previously reported, cavitation is an important source of energy dissipation in rubber toughened epoxies, since cavitation absorbs energy inducing shear yielding in the surrounding matrix (the last mechanism is favored at high filler content, where the surroundings of the particles can efficiently interact with that of the others).

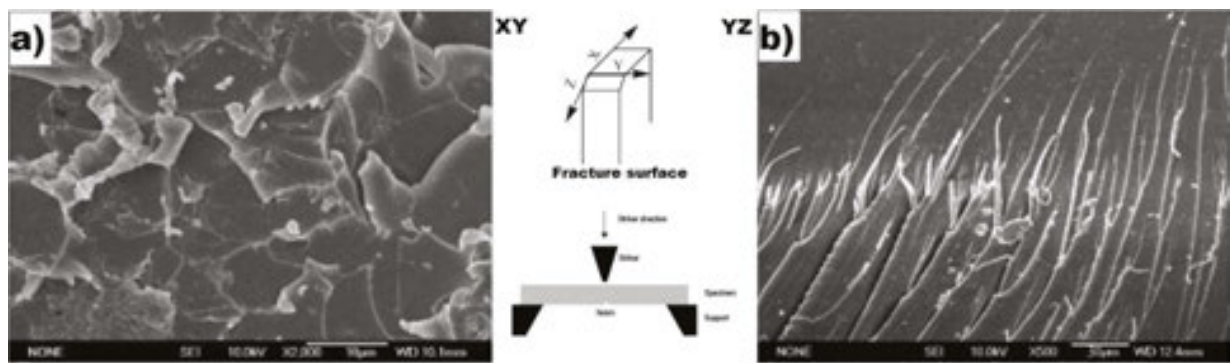


Figure 28. SEM micrographs of the fracture surface in the (a) XY and (b) YZ plane of the HTTE/Epoxy blends [69].

Figure 28(b) reports the SEM micrograph relative to the YZ plane (the region where the crack growth terminated). In this micrograph, the ductile yielding and the consequent fibrillation are evident, which indicate the transition between brittle and ductile states. This transition is in agreement with the large increases of impact strength. The fibril formation mechanism probably consists of the following: (1) voids generated by the debonding between HBP particles and matrix, induce the formation of crazes; (2) after initiation of crazes and voids, the epoxy matrix is elongated under a high tensile stress at the crack-tip region, producing the characteristic fibrils.

Also, Varley et al. [70] demonstrated that the toughening mechanism operating in the HBP/epoxy system is based upon a particle cavitation process. **Figure 29(a)** shows the substantial improvement in fracture toughness (in terms of K_{IC}) with increasing HBP addition.

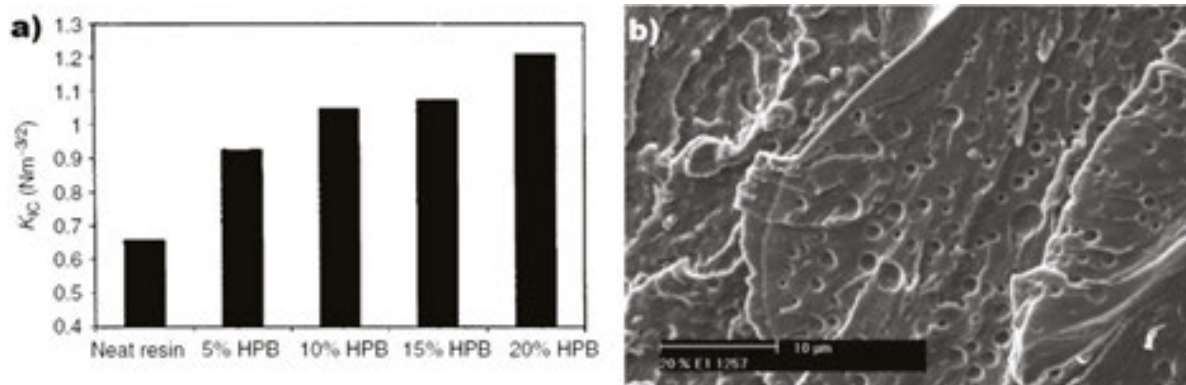


Figure 29. (a) Increase in fracture toughness of the cured resin samples as a function of increasing HBP content and (b) SEM of the 20% HBP/epoxy system [70].

It is noteworthy that this result has been obtained with some decrease in both the T_g and flexural properties. This behavior can be explained in terms of the phase-separated morphology evident from scanning electron micrograph (**Figure 29b**). The size of the HBP particles ($\sim 1\text{--}5 \mu\text{m}$) is of the order suitable to induce toughening mechanisms such as particle cavitation. Interestingly, at the higher levels of HBP concentration the epoxy matrix shows considerable evidence of ductile flow in the continuous epoxy network.

4. Concluding remark

Epoxy adhesives are widely employed in structural applications and the addition of filler is a common method to overcome the brittle nature of this class of polymers. The aim of this contribution was to identify the different mechanisms responsible of the fracture toughening in filled epoxy resins, with special attention to innovative fillers such as graphene nanoplatelets and hyperbranched polymers.

We have reported a classification of the different toughening mechanisms that can occur in a filled epoxy adhesive, based on the filler characteristics. Each filler contributes to the matrix toughening by different mechanisms. In most of the cases, the main occurring mechanisms for filled epoxy systems are crack deflection, matrix deformation, and crack pinning. As the contribution to fracture toughening for each mechanism is indivisible to that of the others, it is not possible to identify the fracture mechanisms only on the basis of the fracture toughness variation. For this purpose, electron microscopy is extensively employed, which allows the identification of the typical features of the searched mechanism in the fracture surface of the toughened epoxy resin. For example, in rubber filled epoxy resins the SEM analysis highlights the presence of small holes, generally larger than the original particles, due to the filler and

matrix cavitation followed by the growth of these voids (cavitation and voiding mechanisms). Crack pinning, common in rigid and thermoplastic particle-toughened epoxy resin, is characterized by tails beyond the particles, caused by the bifurcation of the crack propagation path in the presence of the filler surface, and subsequent meeting of the previously separated crack fronts.

The knowledge of the fracture toughness mechanisms that can occur in toughened epoxy adhesives (and, in general, epoxy resins) allows the development of novel materials able to resist extreme loading conditions, increasing the reliability of the designed final element.

Acknowledgements

This study was financially supported from European Project: EXTREME dynamic loading—pushing the boundaries of aerospace composite material structures—GA 636549.

Author details

Aldobenedetto Zotti, Simona Zuppolini, Mauro Zarrelli* and Anna Borriello

*Address all correspondence to: mauro.zarrelli@cnr.it

Institute of Polymers, Composites and Biomaterials, National Research Council of Italy, Portici, Naples, Italy

References

- [1] Bauer SR, editor. Epoxy Resin Chemistry. Washington, DC: American Chemical Society; 1979. DOI: 10.1021/bk-1979-0114
- [2] Cho YS, Lee HK, Shim MJ, Kim SW. Characteristics of polymer insulator materials: voltage-lifetime characteristics of DGEBA/MDA/SN system. *Materials Chemistry and Physics*. 2000;66(1):70–76. DOI: 10.1016/S0254-0584(00)00272-8
- [3] Kinloch AJ. Toughening epoxy adhesives to meet today's challenges. *MRS Bulletin*. 2003;28(6):445–448. DOI: 10.1557/mrs2003.126
- [4] Quan D, Ivankovic A. Effect of core-shell rubber (CSR) nano-particles on mechanical properties and fracture toughness of an epoxy polymer. *Polymer*. 2015;66(1):16–28. DOI: 10.1016/j.polymer.2015.04.002
- [5] Gojny FH, Wichmann MHG, Kopke UB, Fiedler K. Carbon nanotubereinforced epoxy-composites: enhanced stiffness and fracture toughness at low nanotube content.

- Composites Science and Technology. 2004;64(15):2363–2371. DOI: 10.1016/j.compscitech.2004.04.002
- [6] Zotti A, Borriello A, Zuppolini S, Pomogalio AD, Lesnichaya VA, Zarrelli M. Fabrication and characterization of metal-core carbon-shell nanoparticles filling an aeronautical composite matrix. *European Polymer Journal*. 2015;71:140–151. DOI: 10.1016/j.eurpolymj.2015.07.052
- [7] Wang F, Drzal LT, Qin Y, Huang Z. Enhancement of fracture toughness, mechanical and thermal properties of rubber/epoxy composites by incorporation of graphene nanoplatelets. *Composites: Part A*. 2016;87:10–22. DOI: 10.1016/j.compositesa.2016.04.009
- [8] Anderson TL, Anderson TL. *Fracture Mechanics: Fundamentals and Applications*. 3rd ed. Boca Raton (Florida): Taylor and Francis; 2005. 640 p.
- [9] Selby K, Miller LE. Fracture toughness and mechanical behaviour of an epoxy resin. *Journal of Materials Science*. 1975;10(1):12–24. DOI: 10.1007/BF00541027
- [10] Zotti A, Borriello A, Martone A, Antonucci V, Giordano M, Zarrelli M. Effect of sepiolite filler on mechanical behaviour of a bisphenol A-based epoxy system. *Composites Part B: Engineering*. 2014;67:400–409. DOI: 10.1016/j.compositesb.2014.07.017
- [11] Xavier FF, Xavier R, Àngels S. From curing kinetics to network structure: a novel approach to the modeling of the network buildup of epoxy-anhydride thermosets. *Journal of Polymer Science Part A: Polymer Chemistry*. 2014;52(1):61–75. DOI: 10.1002/pola.26972
- [12] Ma H, Szychaj T, Adamus J. Lewis acid type deep eutectic solvents as catalysts for epoxy resin crosslinking. *RSC Advances*. 2015;5:82813–82821. DOI: 10.1039/C5RA12664A
- [13] Oleinik EF. Epoxy-Aromatic Amine Networks in the Glassy State Structure and Properties. In: Dušek K, editor. *Epoxy Resins and Composites*. 4th ed. Berlin, Heidelberg: Springer; 2005. pp. 49–99. DOI: 10.1007/3-540-16423-5_12
- [14] Shechter L, Wynstra J. Glycidyl ether reactions with alcohols, phenols, carboxylic acids and acid anhydrides. *Industrial and Engineering Chemistry*. 1956;48(1):86–93. DOI: 10.1021/ie50553a028
- [15] Tokizawa M, Okada H, Wakabayashi N. Novel cycloaliphatic epoxy resins. II. Curing reaction with BF₃MEA and its cured properties. *Journal of Applied Polymer Science*. 1993;50:875–884. DOI: 10.1002/app.1993.070500515
- [16] McClintock RM, Hiza MJ. Epoxy resins as cryogenic structural adhesives. *Advances in Cryogenic Engineering*. 1960;3:305–315. DOI: 10.1007/978-1-4684-3105-6_34
- [17] Azeez AA, Rhee KY, Park SJ, Hui D. Epoxy clay nanocomposites-processing, properties and applications: A review. *Composites Part B: Engineering*. 2013;45(1):308–320. DOI: 10.1016/j.compositesb.2012.04.012
- [18] Jajam KJ, Rahman MM, Hosur MV, Tippur HV. Fracture behavior of epoxy nanocomposites modified with polyol diluent and amino-functionalized multi-walled carbon

- nanotubes: a loading rate study. *Composites Part A: Applied Science and Manufacturing*. 2014;59:57–69. DOI: 10.1016/j.compositesa.2013.12.014
- [19] Garg AC, Mai YW. Failure mechanisms in toughened epoxy resins: A review. *Composites Science and Technology*. 1988;31(3):179–223. DOI: 10.1016/0266-3538(88)90009-7
- [20] Kunz-Douglass S, Beaumont PWR, Ashby ME. A model for the toughness of epoxy-rubber particulate composites. *Journal of Materials Science*. 1980;15(5):1109–1123. DOI: 10.1007/BF00551799
- [21] Faber KT, Evans AG. Crack deflection processes—II experiment. *Acta Metallurgica*. 1983;31(4):577–584. DOI: 10.1016/0001-6160(83)90047-0
- [22] Wetzel B, Hauptert F, Zhang MQ. Epoxy nanocomposites with high mechanical and tribological performance. *Composites Science and Technology*. 2003;63(14):2055–2067. DOI: 10.1016/S0266-3538(03)00115-5
- [23] Lange FF. Fracture of Brittle Matrix Particulate Composite. In: Broutman LJ, editor. *Composite Materials, Vol. 5: Fracture and Fatigue*. New York: Academic Press; 1974. pp. 2–44.
- [24] Newman JC, Raju IS. An empirical stress-intensity factor equation for the surface crack. *Engineering Fracture Mechanics*. 1981;15(1–2):185–192. DOI: 10.1016/0013-7944(81)90116-8
- [25] Lange FF. Fracture energy and strength behavior of a sodium borosilicate glass-Al₂O₃ composite system. *Journal of the American Ceramic Society*. 1971;54(12):614–620. DOI: 10.1111/j.1151-2916.1971.tb16016.x
- [26] Moloney AC, Kausch HH, Stieger HR. The fracture of particulate-filled epoxide resins. *Journal of Materials Science*. 1983;18(1):208–216. DOI: 10.1007/BF00543827
- [27] Measurement of Cohesive Parameters of Crazes in Polystyrene Films (Experimental and Applied Mechanics) [Internet]. Available from: <http://what-when-how.com/experimental-and-applied-mechanics/measurement-of-cohesive-parameters-of-crazes-in-polystyrene-films-experimental-and-applied-mechanics/>
- [28] Sultan JN, McGarry FJ. Effect of rubber particle size on deformation mechanisms in glassy epoxy. *Polymer Engineering and Science*. 1973;13(1):29–34. DOI: 10.1002/pen.760130105
- [29] Ismail H, Galpaya D, Ahmad Z. The compatibilizing effect of epoxy resin (EP) on polypropylene (PP)/recycled acrylonitrile butadiene rubber (NBRr) blends. *Polymer Testing*. 2009;28(4):363–370. DOI: 10.1016/j.polymertesting.2008.11.007
- [30] Pearson RA, Yee AF. Influence of particle size and particle size distribution on toughening mechanisms in rubber-modified epoxies. *Journal of Materials Science*. 1991;26(14):3828–3844. DOI: 10.1007/BF01184979

- [31] Chikhi N, Fellahi S, Bakar M. Modification of epoxy resin using reactive liquid (ATBN) rubber. *European Polymer Journal*. 2002;38(2):251–264. DOI: 10.1016/S0014-3057(01)00194-X
- [32] Liu HY, Wang GT, Mai YW, Zeng Y. On fracture toughness of nano-particle modified epoxy. *Composites Part B: Engineering*. 2011;42(8):2170–2175. DOI: 10.1016/j.compositesb.2011.05.014
- [33] Bascom WD, Cottingham RL, Jones RL, Peyser P. The fracture of epoxy- and elastomer-modified epoxy polymers in bulk and as adhesives. *Journal of Applied Polymer Science*. 1975;19(9):2545–2562. DOI: 10.1002/app.1975.070190917
- [34] Sue HJ, Garcia-Meitin EI, Pickelman DM. Literature Review of Epoxy Toughening. In: Arends C, editor. *Polymer Toughening*. New York: CRC Press; 1996. pp. 154–168.
- [35] Arends CB. Design of Tough Epoxy Thermosets. In: Arends CB, editor. *Polymer Toughening*. New York: CRC Press; 1996. pp. 339–380.
- [36] Kinloch AJ, Shaw SJ, Tod DA. Deformation and fracture behaviour of a rubber-toughened epoxy: 1. Microstructure and fracture studies. *Polymer*. 1983;24(10):1341–1354. DOI: 10.1016/0032-3861(83)90070-8
- [37] Yee AF, Pearson RA. Toughening mechanisms in elastomer-modified epoxies: Part 1. *Journal of Materials Science*. 1986;21(7):2462–2474. DOI: 10.1007/BF01114293
- [38] Yee AF, Pearson RA. Toughening mechanisms in elastomer-modified epoxies: Part 2. *Journal of Materials Science*. 1986;21(7):2475–2488. DOI: 10.1007/BF01114294
- [39] Young RJ, Beaumont PWR. Failure of brittle polymers by slow crack growth. *Journal of Materials Science*. 1977;12(4):684–692. DOI: 10.1007/BF00548158
- [40] Lee J, Yee AF. Fracture of glass bead/epoxy composites: on micro-mechanical deformations. *Polymer*. 2000;41(23):8363–8373. DOI: 10.1016/S0032-3861(00)00187-7
- [41] Dillingham RG, Boer FJ. Interphase composition in aluminum/epoxy adhesive joints. *The Journal of Adhesion*. 1987;24(1–2):315–335. DOI: 10.1080/00218468708075434
- [42] Tsai JL, Huang BH, Cheng YL. Enhancing fracture toughness of glass/epoxy composites by using rubber particles together with silica nanoparticles. *Procedia Engineering*. 2011;14:1982–1987. DOI: 10.1016/j.proeng.2011.07.249
- [43] Zhang H, Berglund LA. Deformation and fracture of glass bead/CTBN-rubber/epoxy composites. *Polymer Engineering and Science*. 1993;33(2):100–107. DOI: 10.1002/pen.760330208
- [44] Zotti A, Borriello A, Ricciardi M, Antonucci V, Giordano M, Zarrelli M. Effects of sepiolite clay on degradation and fire behaviour of

- a bisphenol A-based epoxy. *Composites: Part B*. 2015;73:139–148. DOI: 10.1016/j.compositesb.2014.12.019
- [45] Spanoudakis J, Young RJ. Crack propagation in a glass particle-filled epoxy resin. Part 1 effect of particle volume fraction and size. *Journal of Materials Science*. 1984;19(2): 473–486. DOI: 10.1007/BF02403234
- [46] Evans AG. The strength of brittle materials containing second phase dispersions. *Philosophical Magazine*. 1972;26(6):1327–1344. DOI: 10.1080/14786437208220346
- [47] Young RJ, Beaumont PWR. Failure of brittle polymers by slow crack growth. *Journal of Materials Science*. 1975;10(8):1343–1350. DOI: 10.1007/BF00540824
- [48] Kinloch AJ, Maxwell DL, Young RJ. The fracture of hybrid-particulate composites. *Journal of Materials Science*. 1985;20(11):4169–4184. DOI: 10.1007/BF00552413
- [49] Faber KT, Evans AG. Crack deflection processes-I Theory. *Acta Metallurgica*. 1983;31(4): 565–576. DOI: 10.1016/0001-6160(83)90046-9
- [50] Kawaguchi T, Pearson RA. The moisture effect on the fatigue crack growth of glass particle and fiber reinforced epoxies with strong and weak bonding conditions. Part 2. A microscopic study on toughening mechanism. *Composites Science and Technology*. 2004;64(13–14):1991–2007. DOI: 10.1016/j.compscitech. 2004.02.017
- [51] Kinloch AJ, Maxwell D, Young RJ. Micromechanisms of crack propagation in hybrid-particulate composites. *Journal of Materials Science Letters*. 1985;4(10):1276–1279. DOI: 10.1007/BF00723480
- [52] Low IM, Bandyopadhyay S, Silva VM. On hybrid toughened DGEBA epoxy resins. *Polymer International*. 1992;27:131–137.
- [53] Maxwell D, Young RJ, Kinloch AJ. Hybrid particulate-filled epoxy-polymers. *Journal of Materials Science Letters*. 1984;3(1):9–12. DOI: 10.1007/BF00720061
- [54] Pearson RA, Yee AF. Toughening mechanisms in thermoplastic-modified epoxies: 1. Modification using poly(phenylene oxide). *Polymer*. 1993;34(17):3658–3670. DOI: 10.1016/0032-3861(93)90051-B
- [55] Monti M, Rallini M, Puglia D, Peponi L, Torre L, Kenny JM. Morphology and electrical properties of graphene-epoxy nanocomposites obtained by different solvent assisted processing methods. *Composites Part A: Applied Science and Manufacturing*. 2013;46:166–172. DOI: 10.1016/j.compositesa.2012.11.005
- [56] Rafiee MA, Rafiee J, Wang Z, Song H, Yu Z, Koratkar N. Enhanced mechanical properties of nanocomposites at low graphene content. *ACS Nano*. 2009;3(12):3884–3890. DOI: 10.1021/nn9010472

- [57] Hendrick JL, Yilgor I, Wilkes GL, McGrath JE. Chemical modification of matrix resin networks with engineering thermoplastics. *Polymer Bulletin*. 1985;13(3):201–208. DOI: 10.1007/BF00254652
- [58] Cardwel BJ, Yee AF. Toughening of epoxies through thermoplastic crack bridging. *Journal of Materials Science*. 1998;33(22):5473–5484. DOI: 10.1023/A:1004427123388
- [59] Hendrick JL, Yilgor I, Jurek M, Hendrick JC, Wilkes GL, McGrath JE. Chemical modification of matrix resin networks with engineering thermoplastics: 1. Synthesis, morphology, physical behaviour and toughening mechanisms of poly(arylene ether sulphone) modified epoxy networks. *Polymer*. 1991;32(11):2020–2032. DOI: 10.1016/0032-3861(91)90168-I
- [60] Hodgkin JH, Simon GP, Varley RJ. Thermoplastic toughening of epoxy resins: a critical review. *Polymers for Advanced Technologies*. 1998;9(1):3–10. DOI: 10.1002/(SICI)1099-1581(199801)9:1<3::AID-PAT727>3.0.CO;2-I
- [61] Kojima Y, Usuki A, Kawasumi M, Okada A, Kurauchi T, Kamigaito O. Sorption of water in nylon 6-clay hybrid. *Applied Polymer Science*. 1993;49(7):1259–1264. DOI: 10.1002/app.1993.070490715
- [62] Yano K, Usuki A, Okada A. Synthesis and properties of polyimide-clay hybrid films. *Journal of Polymer Science Part A: Polymer Chemistry*. 1997;35(11):2289–2294. DOI: 10.1002/(SICI)1099-0518(199708)35:11<2289::AID-POLA20>3.0.CO;2-9
- [63] Shiu SC, Tsai JL. Characterizing thermal and mechanical properties of graphene/epoxy nanocomposites. *Composites Part B: Engineering*. 2014;56:691–697. DOI: 10.1016/j.compositesb.2013.09.007
- [64] Chandrasekaran S, Sato N, Tolle F, Mülhaupt R, Fiedler B, Schulte K. Fracture toughness and failure mechanism of graphene based epoxy composites. *Composites Science and Technology*. 2014;97:90–99. DOI: 10.1016/j.compscitech.2014.03.014
- [65] Quaresimin M, Schulte K, Zappalorto M, Chandrasekaran S. Toughening mechanisms in polymer nanocomposites: from experiments to modelling. *Composites Science and Technology*. 2016;123:187–204. DOI: 10.1016/j.compscitech.2015.11.027
- [66] Guo QP, Habrard A, Park Y, Halley PJ, Simon GP. Phase separation, porous structure, and cure kinetics in aliphatic epoxy resin containing hyperbranched polyester. *Journal of Polymer Science Part B: Polymer Physics*. 2006;44(6):889–899. DOI: 10.1002/polb.20757
- [67] Ratna D, Varley R, Raman RKS, Simon GP. Studies on blends of epoxy-functionalized hyperbranched polymer and epoxy resin. *Journal of Materials Science*. 2003;38(1):147–154. DOI: 10.1023/A:1021182320285
- [68] Luciani A, Plummer CJG, Nguyen T, Garamszegi L, Manson JAE. Rheological and physical properties of aliphatic hyperbranched polyesters. *Journal of Polymer Science Part B: Polymer Physics*. 2004;42(7):1218–1225. DOI: 10.1002/polb.10671

- [69] Fu JF, Shi LY, Yuan S, Zhang DS, Chen Y, Wu J. Morphology, toughness mechanism, and thermal properties of hyperbranched epoxy modified diglycidyl ether of bisphenol A (DGEBA) interpenetrating polymer networks. *Polymers for Advanced Technologies*. 2008;19(11):1597–1607. DOI: 10.1002/pat.1175
- [70] Varley RJ, Tian W. Toughening of an epoxy anhydride resin system using an epoxidized hyperbranched polymer. *Polymer International*. 2004;53(1):69–77. DOI: 10.1002/pi.1324

IntechOpen

IntechOpen

